

Contents lists available at <http://qu.edu.iq>

Al-Qadisiyah Journal for Engineering Sciences

Journal homepage: <https://qjes.qu.edu.iq>

# Study and analysis of Ti13Nb13Zr implants in the above knee osseointegration prosthesis

Saif M. Abbas<sup>1\*</sup> , Ayad M. Takhakh<sup>2</sup> , Jumaa S. Chiad<sup>2</sup> , and Borhen Louhichi<sup>3</sup> 

<sup>1</sup>Prosthetic and Orthotic Engineering Department, College of Engineering, Al-Nahrain University, Baghdad, Iraq

<sup>2</sup>Mechanical Engineering Department, College of Engineering, Al-Nahrain University, Baghdad, Iraq

<sup>3</sup>Mechanical Engineering Department, College of Engineering, Imam Mohammad Ibn Saud Islamic University (IMSIU), Riyadh 11432, Saudi Arabia

## ARTICLE INFO

### Article history:

Received 14 January 2024

Received in revised form 28 May 2024

Accepted 13 October 2024

### Keywords:

Bone attachment

Femoral bone

Osseointegration

Implants

Ti-13Nb-13Zr alloy

## ABSTRACT

**Introduction:** Osseointegration is a particular kind of prosthesis that is inserted a short titanium rod or screw into the bone surgically and joined to the prosthetic limb. **Experimental part:** This study looked at a patient's gait analysis with above-knee amputation wearing an osseointegration prosthesis implant when walking above a force plate. Evaluated the mechanical and fatigue properties of a Ti13Nb13Zr alloy implant. **Theoretical part:** Drawing and analysis of a femoral bone model with an osseointegration implant using Ansys Workbench 17.2. **Results and discussion:** The results of the tensile testing showed an ultimate tensile strength of 553 MPa, an average yield strength of 480 MPa, an elongation of 19.66%, and a Young's modulus of 2.73 GPa. Furthermore, a compressive strength of 1010 MPa and a compression yield strength of 700 MPa were found by compression testing. The results of fatigue testing, which were displayed as S-N curves, highlighted the alloy's time-dependent fatigue behavior by showing decreasing fatigue strength with an increase in cycles. The force plate showed a maximum force of 600 N was reported. A strong safety margin was shown by Finite Element Analysis in the bone containing the implant, with safety factors often more than 5 and low deformation (2.4 mm) appropriate for prosthetic uses. A good static design was confirmed by the Von-Mises stress distribution, which was primarily below 46 MPa. **Conclusion:** Comprehensive results confirm the mechanical feasibility of the Ti13Nb13Zr alloy for prosthetic applications and offer important new information for improving prosthetic design, guaranteeing durability, and improving safety in practical applications.

© 2024 University of Al-Qadisiyah. All rights reserved.

## 1. Introduction

Patients who have undergone transfemoral amputations have historically been fitted with a prosthesis that includes a socket for the residual limb and some sort of supporting girdle to allow for secure fit and mobility. For several individuals, the use of sockets is hindered by limited range of motion, contact dermatitis or sores, and discomfort during loading or sitting. [1] Furthermore, fit and function issues may arise for individuals with short stumps. Due to these problems, Branemark et al. [2] increased the use of osseointegrated dental implants [3] to replace lost limbs in patients who are not able to wear or utilize a socket.

The proximity of the implant titanium oxide surface and bone tissue without the interposition of fibrous tissues is known as osseointegration [4]. In short, a threaded titanium cylinder, or fixture, is placed in the medullary cavity of the remaining bone during the surgical procedure. Six months of uninterrupted integration are permitted before a skin-penetrating extension (abutment) that acts as an anchor point for the external prosthesis is placed. A thoroughly thought-out rehabilitation program comes next [5]. Since the abutment is not attached to the skin, it may be replaced if it becomes twisted or broken.

\* Corresponding author.

E-mail address: [saif.mohammed@nahrainuniv.edu.iq](mailto:saif.mohammed@nahrainuniv.edu.iq) (Saif M. Abbas)

<https://doi.org/10.30772/qjes.2024.146062.1086>

2411-7773/© 2024 University of Al-Qadisiyah. All rights reserved.



This work is licensed under a [Creative Commons Attribution 4.0 International License](https://creativecommons.org/licenses/by/4.0/).

**Nomenclature:**

<i>SSP</i>	socket-suspended prostheses	<i>FEM</i>	Finite element method
<i>BAP</i>	bone-anchored prosthesis	$\sigma_y$	Yield stress (MPa)
<i>OI</i>	osseointegration implant	$\sigma_{ult}$	Ultimate stress (MPa)
<i>OPRA</i>	Osseointegrated prostheses for the Rehabilitation of Amputees	<i>E</i>	Modules of elasticity (GPa)
<i>ILP</i>	Integral leg prosthesis	<i>CS</i>	Compressive Strength
<i>ASTM</i>	American Society for Testing and Materials Information	<i>YSc</i>	Compression Yield Strength
<i>GRF</i>	Ground reaction force		

The technique reduces socket-caused skin problems, improves quality of life, and improves prosthesis handling and limb control in a subset of amputation patients (mostly due to trauma and tumors) [6, 7, 8]. Diabetes, rheumatoid arthritis, renal failure, malnourishment, immunosuppression, wound infection, and *S aureus* nasal carriage are risk factors for prosthetic joint infections [9-11]. It has been demonstrated that obesity poses a separate risk for periprosthetic infection [12]. Diabetes seems to hinder osseointegration, and smoking is harmful to bone repair [13-16]. A good substitute for socket-suspended prostheses (SSP) for amputee patients who experience discomfort, pressure sores, and limited mobility is a bone-anchored prosthesis (BAP) that uses an osseointegration implant (OI). In [17]. An OI has the benefit of giving an artificial limb a direct skeletal connection. In [18] This eliminates the socket-residuum interface and all of its related issues while also improving walking and sitting conditions, improving Osseo's perception, and producing more physiological and stable prosthetic control [19-22]. There are now two commercially available OI systems. The titanium screw fixation system, which was created by the Swedish Branemark group and is marketed as the Osseointegrated prostheses for the Rehabilitation of Amputees Implant system (OPRA) by Integrum AB Sweden, is the oldest and has the longest follow-up assessments.[23] The press-fit attachment technique, created and utilized by German, Dutch, and Australian osseointegration organizations, is a second, somewhat more modern OI system. It is offered as the Integral leg prosthesis (ILP) Osseointegrated femur or tibia prosthesis. [24–28] Press-fit implants need less time to treat overall than screw-type implants, which means that using a press-fit implant will significantly reduce the amount of time needed to reach full weight bearing. In [29] Press-fit implants have a somewhat higher femoral OI survival rate than screw implants, according to a recent systematic analysis of the safety of BAP [30]. Numerous researches have demonstrated superior performance metrics between BAP and SSP, resulting in higher levels of function, activity, and health-related quality of life.[31] This study aimed to assess the mechanical and fatigue characteristics of a Ti13Nb13Zr alloy implant, analyze the walking gait in a patient with above-knee amputation featuring osseointegration, and examine a femoral bone model with an osseointegration implant using Ansys Workbench 17.2.

## 2. Experimental procedures

The study's main objectives are to create and analyze samples for prosthetic osseointegration implants above the knee and to assess the patient's gait cycle.

### 2.1. Material selection for the Implant

As indicated in Fig. 1, cylindrical pieces of the Ti-13Nb-13Zr ASTM F-1713 [32] alloy that is investigated and used by many researchers [33-34]. A 400 mm in length and 13 mm in diameter were provided for the experiments. These samples were obtained from Shaanxi Yuzhong Industry Development Co. in Baoji, China, in order to establish standardized specimens for mechanical testing, specifically to examine tensile, compressive, and fatigue characteristics.

The proper geometries were created using the Wire Electrical Discharge Machining process. A CNC lathe ST-10 and a CNC milling machine VF-1 from Haas Automation Inc., located in Oxnard, California, were then used to make and modify prefabricated rods of a lower size to the required specifications. Table 1 provides a detailed description of the chemical composition of the Ti-13Zr-13Nb alloy by using XRF testing.



**Figure 1.** The Ti-13Zr-13Nb specimen

**Table 1.** Ti-13Zr-13Nb Base Alloy's chemical composition (wt%)

Elements	wt. pct. %
Zr	15.220
Nb	13.450
Fe	00.115
Mo	00.077
Zn	00.053
Mn	00.039
Cu	00.043
Ti	69.940
Residual Element	00.135
Sum of concentration	99.000

### 2.2. Tensile test device

The mechanical properties of the materials used for manufacturing osseointegration implants are evaluated using a tensile test device as shown in Figure 2.



**Figure 2.** Tensile test setup

The ASTM E8/E8M standard is a vital tool for evaluating the tensile properties of metallic materials, including titanium alloys like Ti13Nb13Zr, such as yield strength, ultimate tensile strength, elongation, and area reduction for assessing the material's reaction to stress, giving insight into its mechanical capability, durability, and suitability for prosthetic limbs. As seen in Fig. 3, the tensile characteristics of Ti13Nb13Zr are determined by testing that follows ASTM E8/E8M-16a [35].

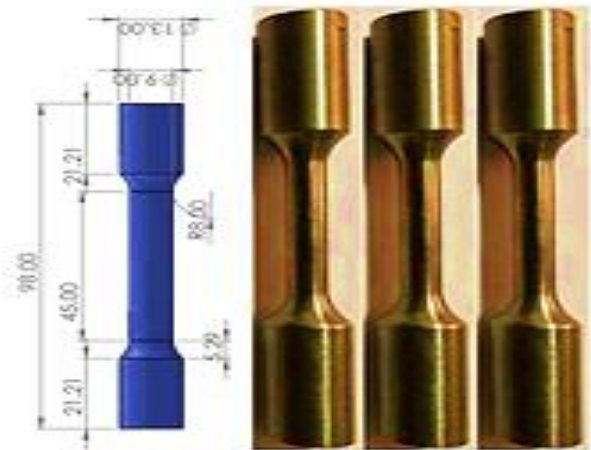


Figure 3. Tensile test specimen for Ti-13Nb-13Zr

### 2.3. Compression test device

The compression test device as shown in Fig. 4 is used to test the compressive strength of Ti-13Nb-13Zr alloy by compressing a specimen to measure its axial load capacity, deformation characteristics, and compressive strength. The main purpose is to compress Ti-13Nb-13Zr alloy to get useful information on their strength, structural integrity, and resistance to compressive pressures. This test was implemented at The Iraqi Ministry of Science and Technology in Baghdad A Ti 13Nb13Zr specimen was subjected to a static compression test in compliance with ASTM E9-09[36] standards. Up until it broke or fractured, the sample was subjected to the test at a steady traversal speed of 2 mm/min. The objective was to assess the material's compressive strength and behavior under these specific testing conditions. This process was carried out on three samples in total. Fig. 5 shows the specimen's dimensions that were used in the compression test.



Figure 4. Compression test machine



Figure 5. Compression specimen for Ti-13Nb-13Zr

### 2.4. Rotating Fatigue Test

A fatigue test of specimen made of the Ti13Nb13Zr alloy is usually carried out by applying cyclic, repeating stresses, as Fig. 6 It helps comprehend how long a material can sustain the pressures brought on by rotational motion, which is important information for engineering and design decisions.



Figure 6. Fatigue test

As well as this type of application may effect by fracture of different mode [37] was utilized to create the S-N curve for human bone. Samples were subjected to alternating compressive and tensile loads using a particular testing technique, with an average stress of zero each cycle. The data, shown in Fig. 7, was graphed and analyzed using Microsoft Excel in order to determine a link between stress (S) and the number of cycles to failure (N). Ages and gender differences in the sample were explained by the average number of cycles that resulted in failure at particular stress levels. To determine fatigue life, predictive analysis was performed using the mean curve.

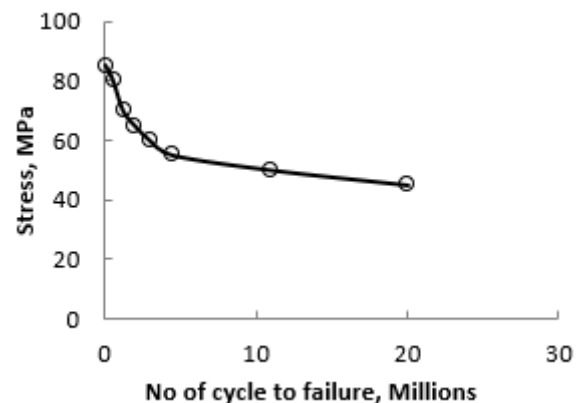


Figure 7. The S-N curve for the human bone [35]

The fact that cadaveric bone was used to develop these S-N correlations means that predictions might not accurately represent bone function in vivo. It is advisable to exercise caution as these estimations, which provide extremely conservative predictions for fatigue life, may not exactly reflect circumstances found in living bone.

## 2.5. Experimental Evaluation of Loads

As part of the experimental work, the patient depicted in Figure 8 was analyzed on a force plate at prosthetics and orthotics engineering department with the College of Engineering at Al-Nahrain University's ethical consent (02/2020), the patient's information included height 1.70 meters, gender male, right-side above-knee amputation, and weight 80 kg. The goal was to find the curve load- time and maximum GRF used in various walking scenarios on the prosthetic osseointegration limb. So that the magnitude of maximum force can be used in Finite Element Modeling (FEM) with software of ANSYS 17.2 to examine the overall deformation and stress distribution of the implant and bone [40-42].



**Figure 8.** Above-knee osseointegration prosthesis

## 2.6. 3D Modeling and FEM Model

The model prosthetic implant as shown in Fig. 9 can be divided into two parts:

1. Fixed Intramedullary Stem: The residual limb, or portion of the leg left following amputation, is intended to have this prosthetic device implanted into its medullary canal. Usually made of a biocompatible material, the prosthesis is stabilized and supported by the intramedullary stem.
2. Transcutaneous Part (Abutment): This part acts as the interface between the prosthetic and natural limbs, joining the intramedullary stem and going through the skin. The prosthetic components are firmly attached to the intramedullary stem by the abutment, which guarantees a strong connection.

Analyzing, customizing, and visualizing prosthetic design is made possible by the Solid Works model of the implant and bone. Using this program, scientists and engineers may precisely modify the implant's size to guarantee the best possible fit, biomechanical compatibility, and general

usefulness for patients who have had above-knee amputations. Making use of this technology enables the prosthetic design to be precisely modified and improved, enhancing its functioning and better meeting the demands of each user individually.

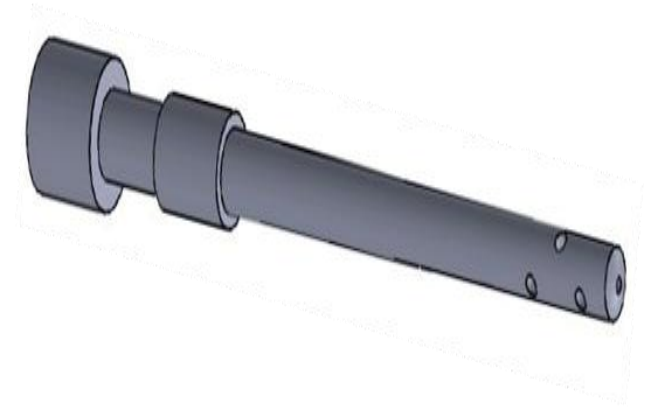


**Figure 9.** The model of the prosthetic implants

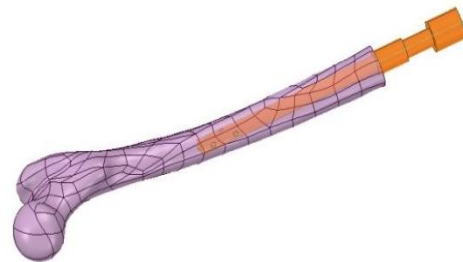


**Figure 10.** The model of the implant with different length

The meshing of the implant and femoral bone utilized ten-node tetrahedral elements, (nodes 9106 and element 4984) specifically the SOLID187 element type Fig. 11. These elements are commonly employed in finite element modelling (FEM) analysis to discretize and approximate the geometry of solid structures. This approach aids in simulating and understanding stress and deformation behaviors within prosthetic systems.



**Figure 11.** Meshed model with ten-node tetrahedral elements

Surface-to-surface contact components were used to help the prosthesis and bone make contact, TARGE170 and CONTA174 in particular. These components make it easier to simulate the interactions between different model pieces, enabling the consideration of forces and contact behavior in the mechanical interaction between the prosthesis and the bone as well as in the load transmission. Boundary constraints which include solid support at the implant and an applied load that reflects the patient's weight at the proximal end of the femur are incorporated into the model's analysis, as



shown in Fig. 12. These critical boundary conditions are necessary in order to model and assess how the prosthetic system will behave and operate in certain loading and support scenarios. Table 2 displays the mechanical characteristics of cortical bone.

**Table 2.** Mechanical properties of the cortical bone [38]

Sample (MPa)	$\sigma_y$ (MPa)	$\sigma_{ult}$ (MPa)	E (GPa)
Cortical bone	175	205	20

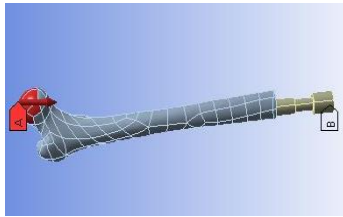


**Figure 12.** Boundary condition of model

### 3. Results and Discussion

#### 3.1. Tensile properties results for metallic material

This study's mechanical characteristics show a typical curve for materials with proof stress, particularly when stress is measured at the 0.2% plastic deformation limit. The ASTM-recommended static tensile testing procedure was used to the Ti-13Nb-13Zr alloy samples. These findings are reported in Table 3 along with comparisons to the supplier's certificate and ASTM F1713 standards [39]. By comparing the material to standards and specifications, these comparisons play a critical role in assessing the material's appropriateness for biomedical engineering prosthetic applications and determining if it satisfies the mechanical criteria for usage in biological prosthesis. In actuality, the study's findings almost exactly matched the manufacturer's standards. From the compression and tensile tests, the stress-strain curves showed the usual properties of materials without a clear yield point.

#### 3.2. Compression properties results

When the parameters Compressive Strength (CS) and Compression Yield Strength (YSc) were evaluated, the static compression test yielded the following values: It was determined that CS was 1010 MPa and YSc was 700 MPa with comparison with ref [39]. The typical compression stress-strain curves seen in Fig. 14 reveal the great strength and excellent ductility of the Ti-13Nb-13Zr alloy. Biomedical applications require materials with these properties, particularly for prosthetic components that must be able to withstand heavy loads without losing their structural integrity. Understanding how the material responds to compressive stresses experienced when performing weight-bearing duties like standing or walking depends on the findings of the Ti-13Nb-13Zr compression test. Materials associated to implants, particularly osseointegrated prosthetic components, must possess adequate compressive strength to withstand these kinds of stresses without breaking down or deforming. The results of the Ti-13Nb-13Zr compression test confirm the material's resistance to mechanical pressures found in biological applications. This helps to guarantee the efficacy and dependability of prosthetic implants by enhancing their robustness, safety, and compatibility with bone.

**Table 3.** Mechanical properties of Ti-13Nb-13Zr alloy

Sample	$\sigma_y$ (MPa)	$\sigma_{ult}$ (MPa)	E (GPa)
1	470.562	556.5	2.4188
2	503.103	543.73	2.7589
3	472.235	554.4	2.7312

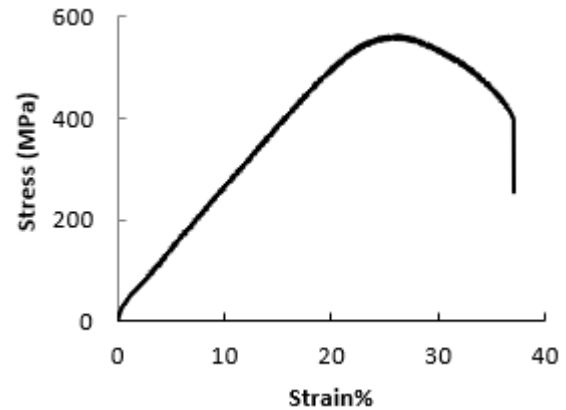


**Figure 13.** Average stress-strain curve for implant material

**Table 4.** Compression of Ti-13Nb-13Zr alloy result

Sample	YSc (MPa)	$\sigma_{ult}$ (MPa)
1	1010	700
2	1012	705
3	1008	702

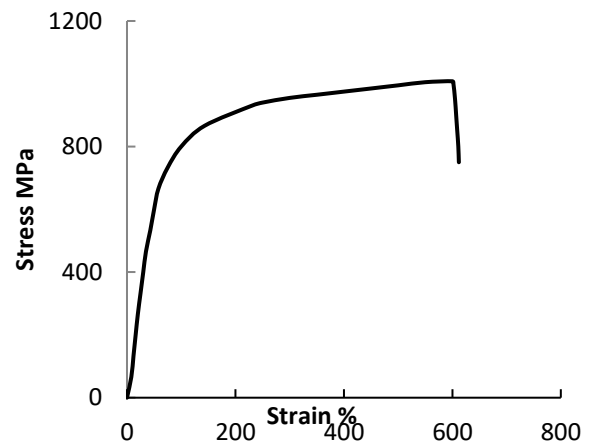


**Figure 14.** Average compression stress-strain curve for implant material

### 3.3. Fatigue property results for metallic material

The fatigue testing was done at room temperature with tensions ranging from 400 MPa to 250 MPa. Fig. 15 displays the S-N curves discovered throughout these tests. Based on the results of the tensile test, the sample had the best fatigue qualities across all the conditions evaluated, which is in line with the findings. Interestingly, the fatigue strength of the Ti-13Nb-13Zr implant samples decreased steadily as the number of cycles to failure increased. This pattern points to a gradual loss of the material's fatigue resistance and the results showed that it is close to the reference [40]. Understanding how the material behaves under cyclic stress and how long it can tolerate fatigue are critical to ensuring the continuous functionality of prosthetic implants in long-term, real-world applications.

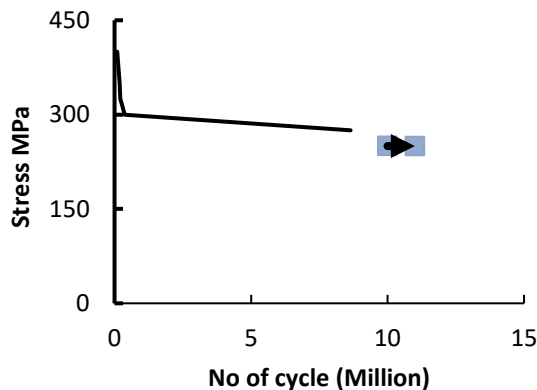


Figure 15. S-N curve for Ti-13Nb-13Zr alloy

### 3.4. Force Plate Results.

Analyzing the ground reaction force applied on an abutment of an osseointegrated prosthesis implant through a force plate during a patient's gait cycle gives information about the prosthetic osseointegration loading. Emphasizing peak pressures during heel contact and toe-off is crucial, allowing clinicians to discern potential asymmetries between the right and left legs. An extensive analysis of the implant's abutment loading circumstances is made possible by closely examining peak force and moment values during particular gait phases. This examination helps evaluate the stability and functioning of the implant during the course of the gait cycle. A visual aid is provided by the left and right legs, represented by red and green lines in Fig. 16, which shows force curves over time. The 600 N maximum force that was collected offers a dynamic picture that shows the stress dynamics of the implant at various stages of the gait cycle.

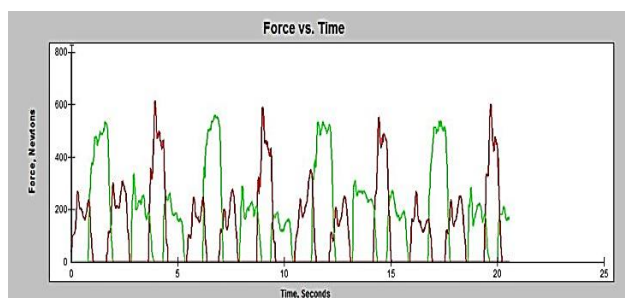


Figure 16. Force vs. Time

### 3.5. FEM Analysis Results

In biomechanical engineering, analyzing a prosthetic model with the ANSYS Workbench software (version 17.2) yields the total deformation, equivalent stress (Von-Mises), and safety factor as conventional procedures. The safety factors for the bone with implant model, obtained from the results of the numerical analysis, are shown in Fig. 17. The bulk of implanted bone, according to the study, is found in the blue and green zones, where the safety factor is more than 5, far higher than the required value of 1.25. A little area of the prosthetic model's bottom side has a safety factor of less than 5.

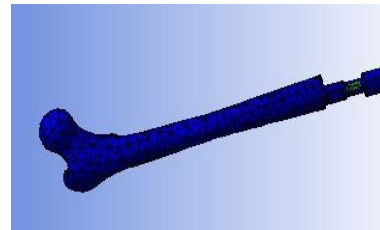


Figure 17. Fatigue factor of safety

The Von-Mises stress for the implanted bone model is 46 MPa and shown in Fig. 18. When compared to the yield stress (470 Mpa and 175 Mpa for the implant material and bone, respectively), which is less than for the implant material and bone, it can be concluded that the static design is good.

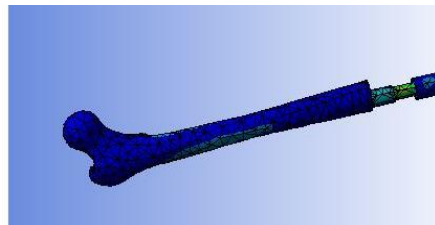


Figure 18. Equivalent stress (von Mises)

Fig. 19. The total deformation of the implant model in the bone. The total deformation research indicates that the maximum deformations (2.4 mm) are appropriate for applications using prosthetic models.

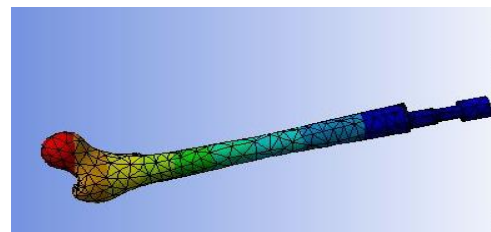


Figure 19. Total deformation

## 4. Conclusions

1. The Ti13Nb13Zr alloy had excellent compressive and tensile strength, demonstrating its mechanical suitability for use in prosthetic applications. The results of the tensile test showed that the material had an ultimate tensile strength of 553 MPa, average yield strength of

480 MPa, an elongation of 19.66%, and a Young's modulus of 2.73 GPa.

2. Compression testing confirmed the alloy's capacity to bear weight by demonstrating a compressive strength of 1010 MPa and a compression yield strength of 700 MPa.
3. The alloy's time-dependent fatigue behavior was emphasized by fatigue testing, as shown by S-N curves, underscoring the necessity of gaining a complete grasp of the alloy's behavior over prolonged cycles.
4. Gait Analysis: Force plate data obtained throughout the gait cycle provided insights into the moments and ground response pressures on the implant's abutment, helping to assess implant loading patterns. A maximum force of 600 N was reported.
5. The results of Finite Element Analysis demonstrated a strong safety margin in the implanted bone, with safety factors regularly more than 5 and minimum deformation (2.4 mm) appropriate for prosthetic use.
6. The alloy's use in prosthetic systems is supported by the Von-Mises stress distribution, which was mostly found to be below 46 MPa and confirms a good static design.
7. Comprehensive results confirm the mechanical feasibility of the Ti13Nb13Zr alloy for prosthetic applications and offer important new information for improving prosthetic design, guaranteeing durability, and improving safety in practical applications.

### Authors' contribution

All authors contributed equally to the preparation of this article

### Declaration of competing interest

The authors declare no conflicts of interest.

### Funding source

This study didn't receive any specific funds.

### Data availability

The data that support the findings of this study are available from the corresponding author upon reasonable request.

### Acknowledgments

The authors would like to acknowledge Al-Nahrain University for its continuous support to improve the research quality.

### REFERENCES

- [1] Transfemoral amputation: a survey of quality of life, prosthetic use and problems. *Prosthet Orthot Int.* 25:186–194, 2001. <https://doi.org/10.1080/03093640108726601>
- [2] Branemark R, Branemark PI, Rydevik B, Myers RR. Osseointegration in skeletal reconstruction and rehabilitation: a review. *J Rehabil Res Dev.* 38:175–181, 2001. <https://doi.org/10.1682/jrrd.2003.07.0107>
- [3] Thesle, A.; Brånemark, R.; Håkansson, B.; Ortiz-Catalan, M. Biomechanical Characterisation of Bone-anchored Implant Systems for Amputation Limb Prostheses: A Systematic Review. *Ann. Biomed. Eng.* 2018, 46, 377–391. <https://doi.org/10.1007/s10439-017-1976-4>
- [4] Al Muderis M, Khemka A, Lord SJ, Van de Meent H, Frolke JPM. Safety of osseointegrated implants for transfemoral amputees: a two-center prospective cohort study. *J Bone Joint Surg.* 2016; 98(11):900–9. <https://doi.org/10.2106/jbjs.15.00808>
- [5] Hagberg K, Branemark R. One hundred patients treated with osseointegrated transfemoral amputation prostheses: rehabilitation perspective. *J Rehabil Res Dev.* 46:331–344, 2009. <https://doi.org/10.1682/jrrd.2012.08.0135>
- [6] Hagberg K, Hansson E, Branemark R. Outcome of percutaneous osseointegrated prostheses for patients with unilateral transfemoral amputation at two-year follow-up. *Arch Phys Med Rehabil.* 95:2120–2127, 2014. <https://doi.org/10.1016/j.apmr.2014.07.009>
- [7] Lundberg M, Hagberg K, Bullington J. My prosthesis as a part of me: a qualitative analysis of living with an osseointegrated prosthetic limb. *Prosthet Orthot Int.* 35:207–214, 2011. <https://doi.org/10.1177/0309364611409795>
- [8] Van de Meent H, Hopman MT, Frolke JP. Walking ability and quality of life in subjects with transfemoral amputation: a comparison of osseointegration with socket prostheses. *Arch Phys Med Rehabil.* 94:2174–2178, 2013. <https://doi.org/10.1177/0309364611409795>
- [9] Berbari EF, Hanssen AD, Duffy MC, Steckelberg JM, Ilstrup DM, Harmsen WS, Osmon DR. Risk factors for prosthetic joint infection: case-control study. *Clin Infect Dis.* 27:1247–1254, 1998. <https://doi.org/10.1086/514991>
- [10] Saif M. Abbas and Ammar I. Kubba (2020) Fatigue Characteristics and Numerical Modelling Prosthetic for Chopart Amputation Modelling and Simulation in Engineering Volume 2020, Article ID 4752479. <https://doi.org/10.1155/2020/4752479>
- [11] S.M. Abbas, Fatigue Characteristics and Numerical Modeling Socket for Patient with Above Knee Prosthesis, Defect and Diffusion Forum Journal Vol. 398, (2020) 76-82. <https://doi.org/10.4028/www.scientific.net/ddf.398.76>
- [12] Namba RS, Paxton L, Fithian DC, Stone ML. Obesity and perioperative morbidity in total hip and total knee arthroplasty patients. *J Arthroplasty.* 20 (7 suppl 3):46–50, 2005. <https://doi.org/10.1016/j.arth.2005.04.023>
- [13] Baig MR, Rajan M. Effects of smoking on the outcome of implant treatment: a literature review. *Indian J Dent Res.* 18:190–195, 2007. <https://doi.org/10.4103/0970-9290.35831>
- [14] Hasegawa H, Ozawa S, Hashimoto K, Takeichi T, Ogawa T. Type 2 diabetes impairs implant osseointegration capacity in rats. *Int J Oral Maxillofac Implants.* 23:237–246, 2008. <https://doi.org/10.11607/jomi.3480>
- [15] Mellado-Valero A, Ferrer Garcia JC, Herrera Ballester A, Labaig Rueda C. Effects of diabetes on the osseointegration of dental implants. *Med Oral Patol Oral Cir Bucal.* 12:E38–43, 2007. <https://doi.org/10.4317/medoral.15.e52>
- [16] Sloan A, Hussain I, Maqsood M, Eremín O, El-Sheemy M. The effects of smoking on fracture healing. *Surgeon.* 8:111–116, 2010. <https://doi.org/10.1016/j.surge.2009.10.014>
- [17] Leijendekkers RA, van Hinte G, Frolke JP, van de Meent H, Nijhuis-van der Sanden MW, Staal JB. Comparison of bone-anchored prostheses and socket prostheses for patients with a lower extremity amputation: a systematic review. *Disabil Rehabil.* 39(11):1045–58, 2017. <https://doi.org/10.1080/09638288.2016.1186752>
- [18] Branemark R, Branemark PI, Rydevik B, Myers RR. Osseointegration in skeletal reconstruction and rehabilitation: a review. *J Rehabil Res Dev.* 38(2):175–81, 2001. <https://doi.org/10.1682/jrrd.2003.07.0107>
- [19] Overmann AL, Aparicio C, Richards JT, Mutreja I, Fischer NG, Wade SM, et al. Orthopaedic osseointegration: Implantology and future directions. *J Orthop Res.* 2020;38(7):1445–54. <https://doi.org/10.1002/jor.24576>
- [20] Hagberg K, Hansson E, Branemark R. Outcome of percutaneous osseointegrated prostheses for patients with unilateral transfemoral amputation at two-year follow-up. *Arch Phys Med Rehabil.* 95(11):2120–7, 2014. <https://doi.org/10.1016/j.apmr.2014.07.009>
- [21] Leijendekkers RA, van Hinte G, Frolke JP, van de Meent H, Atsma F, Nijhuis-van der Sanden MW, et al. Functional performance and safety of bone-anchored prostheses in persons with a transfemoral or transtibial amputation: a prospective one-year follow-up cohort study. *Clin Rehabil.* 33(3):450–64, 2019. <https://doi.org/10.1177/0269215518815215>
- [22] Van de Meent H, Hopman MT, Frolke JP. Walking ability and quality of life in subjects with transfemoral amputation: a comparison of

- osseointegration with socket prostheses. Arch Phys Med Rehabil. 94(11):2174–8, 2013. <https://doi.org/10.1016/j.apmr.2013.05.020>
- [23] Pitkin M. Design features of implants for direct skeletal attachment of limb prostheses. J Biomed Mater Res A. 101(11):3339–48, 2013. <https://doi.org/10.1002/jbm.a.34606>
- [24] Hagberg K, Ghassemi Jahani SA, Kulbacka-Ortiz K, Thomsen P, Malchau H, Reinholdt C. A 15-year follow-up of transfemoral amputees with bone-anchored transcutaneous prostheses. Bone Joint J. 102-B(1):55–63, 2020. <https://doi.org/10.1302/0301-620X.102B1.BJJ-2019-0611>
- [25] Al Muderis M, Khemka A, Lord SJ, Van de Meent H, Frolke JP. Safety of Osseointegrated Implants for Transfemoral Amputees: A Two-Center Prospective Cohort Study. J Bone Joint Surg Am. 98 (11):900–9, 2016. <https://doi.org/10.2106/JBJS.15.00808>
- [26] Al Muderis M, Lu W, Li JJ. Osseointegrated Prosthetic Limb for the treatment of lower limb amputations: Experience and outcomes. Unfallchirurg. 120(4):306–11, 2017. <https://doi.org/10.1007/s00113-016-0296-8>
- [27] Aschoff H. About osseointegrated, percutaneous implants for rehabilitation following limb-amputation Langenbecks Arch Surg Conference publication. Paper number 13 (pp903), 2014. <https://doi.org/10.29199/cann.101015>
- [28] Aschoff HH, Kennon RE, Keggi JM, Rubin LE. Transcutaneous, distal femoral, intramedullary attachment for above-the-knee prostheses: an endo-exo device. J Bone Joint Surg Am. 92 Suppl 2:180–6, 2010. <https://doi.org/10.2106/JBJS.J.00806>
- [29] Hagberg K, Branemark R. One hundred patients treated with osseointegrated transfemoral amputation prostheses—rehabilitation perspective. J Rehabil Res Dev. 46(3):331–44, 2009. <https://doi.org/10.1682/jrrd.2012.08.0135>
- [30] Atallah R, Leijendekkers RA, Hoogeboom TJ, Frolke JP. Complications of bone-anchored prostheses for individuals with an extremity amputation: A systematic review. PLoS One. 13(8) 0201821, 2018. <https://doi.org/10.1371/journal.pone.0201821>
- [31] Hagberg K, Branemark R, Gunterberg B, Rydevik B. Osseointegrated trans-femoral amputation prostheses: prospective results of general and condition-specific quality of life in 18 patients at 2-year followup. Prosthet Orthot Int. 32(1):29–41, 2008. <https://doi.org/10.1080/03093640701553922>
- [32] Standard Specification for Wrought Titanium-13Niobium-13Zirconium Alloy for Surgical Implant Applications R58130 Designation: F1713 – 08 2013. <https://doi.org/10.1520/f1713-08r21e01>
- [33] Schneider, S.G. [et al]. Mechanical properties and cytotoxic evaluation of the Ti-3Nb-13Zr alloy. Biomecánica, 2000, vol. 8, núm. 1, p. 84-87. UR <http://hdl.handle.net/2099/5423 DOI10.5821/sibb.v8i1.1653>
- [34] Fahem, A.F., Guthai, A.T. & Mosa, M.H. Enhancing Specimen Grip in Torsional Split Hopkinson Bar to Characterize Engineering Materials Under Pure Torsional Load. Exp Tech (2024). <https://doi.org/10.1007/s40799-024-00719-8>
- [35] American Society for Testing and Materials Information, Standard Test Methods for Tension Testing of Metallic Materials Designation: E8/E8M – 16a.
- [36] American Society for Testing and Materials Information, Standard Test Methods of Compression Testing of Metallic Materials at Room Temperature Designation: E 9 – 89a, 2000.
- [37] Fahem, A., Kidane, A. & Sutton, M. Loading Rate Effects for Flaws Undergoing Mixed-Mode I/III Fracture. Exp Mech 61, 1291–1307 (2021). <https://doi.org/10.1007/s11340-021-00739-0>
- [38] Perez, A.; Mahar, A.; Negus, C.; Newton, P.; Impelluso, T. A. Computational evaluation of the effect of intramedullary nail material properties on the stabilization of simulated femoral shaft fractures. Med. Eng. Phys. 30, 755–760, 2008. <https://doi.org/10.1016/j.medengphy.2007.08.004>
- [39] American Society for Testing and Materials Information, Standard Designation: F1713 – 08 (Reapproved 2013). Specification for Wrought Titanium-13Niobium-13Zirconium Alloy for Surgical Implant Applications (UNS R58130). <https://doi.org/10.1520/f1713-08>
- [40] Libo Zhou, Tiechui Yuan, Ruidi Li, Jianzhong Tang, Guohua Wang, Kaixuan Guob and Jiwei Yuan. Densification, microstructure evolution and fatigue behavior of Ti-13Nb-13Zr alloy processed by selective laser melting. Powder Technology 342 (2019) 11–23. <https://doi.org/10.1016/j.powtec.2018.09.073>.
- [41] Fahem, A., A. Alshamma, F. (2009). 'A study of the effect of impact loading on dsifs and crack propagation in plate', *Al-Qadisiyah Journal for Engineering Sciences*, 2(2), pp. 288-303. <https://doi.org/10.30772/qjes.2009.34785>
- [42] Moaveni Saeed. 2008. Finite Element Analysis : Theory and Application with Ansys. 3rd ed. Upper Saddle River N.J: Pearson Prentice Hall.